Original Article

The potential role of breast MRI in evaluation of triple-negative breast cancer and fibroadenoma of less than 3 cm

Zifan Wei[1,2#], Xue Chen[3#], Yiwen Yang[1], Ling Yang[1], Xinxing Ma[1]^

[1]Department of Radiology, The First Affiliated Hospital of Soochow University, Suzhou, China; [2]Department of Medical Imaging Science, Suzhou Medical College of Soochow University, Suzhou, China; [3]Department of Radiology, The Affiliated Suzhou Hospital of Nanjing Medical University, Suzhou Municipal Hospital, Suzhou, China

Contributions: (I) Conception and design: X Ma; (II) Administrative support: L Yang; (III) Provision of study materials or patients: X Ma; (IV) Collection and assembly of data: Z Wei, X Chen; (V) Data analysis and interpretation: Z Wei, X Chen, Y Yang; (VI) Manuscript writing: All authors; (VII) Final approval of manuscript: All authors.

[#]These authors contributed equally to this work.

Correspondence to: Xinxing Ma, MD, PhD. Department of Radiology, The First Affiliated Hospital of Soochow University, 188 Shizi Street, Suzhou 215006, China. Email: xinxingma@suda.edu.cn.

Background: The majority of small-sized (<3 cm) triple-negative breast cancer (TNBC) exhibit smooth margins upon palpation and are often oval or rounded masses. Distinguishing these masses preoperatively from fibroadenomas (FAs) would be very meaningful for clinical practice. The aim of our study was to evaluate the magnetic resonance imaging (MRI) appearance of TNBC and differentiate it from FAs.

Methods: In this retrospective single-center study, we included 37 patients with TNBCs and 36 patients with FAs who underwent breast MRI. We employed the χ^2 test and *t*-test to compare the differences in morphological features, dynamic contrast-enhanced MRI (DCE-MRI) parameters, and apparent diffusion coefficient (ADC) values between the two groups. Additionally, we constructed non-parametric receiver operating characteristic (ROC) curves using ADC values, with pathological results serving as the gold standard.

Results: A total of 37 TNBC lesions and 39 FA lesions were included in the final analysis. TNBCs exhibited more frequent irregular shape, irregular margins, peritumoral edema, fast enhancement in the initial phase, rim enhancement, and time-signal intensity curve (TIC) type III compared to FAs (all P<0.05). Conversely, low-signal segregation in T2-weighted imaging (T2WI) and TIC type I were commonly found in FAs. The mean ADC value of TNBCs was significantly lower than that of FAs [$(1.104\pm0.13)\times10^{-3}$ *vs.* $(1.613\pm0.16)\times10^{-3}$ mm^2/s, P<0.05]. The cutoff ADC for differentiating TNBCs from FAs was 1.239×10^{-3} mm^2/s, yielding an area under the curve (AUC) of 0.997, a sensitivity of 94.6%, and a specificity of 100%.

Conclusions: The morphological presentation of MRI, internal enhancement features of the mass, TIC curves, and ADC values provide valuable differential diagnostic information for TNBC and FA masses with a maximum diameter of less than 3 cm.

Keywords: Triple-negative breast cancer (TNBC); fibroadenoma (FA); magnetic resonance imaging (MRI); apparent diffusion coefficient (ADC); time-signal intensity curve (TIC)

Submitted Mar 26, 2024. Accepted for publication Jul 11, 2024. Published online Aug 27, 2024.
doi: 10.21037/tcr-24-498
View this article at: https://dx.doi.org/10.21037/tcr-24-498

^ ORCID: 0009-0009-7263-9106.

Introduction

Triple-negative breast cancer (TNBC) represents a distinct subtype of breast cancer characterized by the absence of progesterone receptors (PR), estrogen receptors (ER), and human epidermal growth factor receptor-2 (HER-2) (1). TNBC exhibits a highly malignant behavior, with a propensity for recurrence and metastasis due to the lack of specific targets for endocrine therapy and HER-2 treatment (2). Notably, the majority of small-sized (<3 cm) TNBCs exhibit smooth margins upon palpation and are often oval or rounded masses (3,4). Distinguishing these masses preoperatively from fibroadenomas (FAs) poses a challenge (5-7). Yet, early preoperative detection and accurate diagnosis are critical for selecting appropriate treatment strategies and assessing patient prognosis in TNBC cases. As breast malignant tumors, TNBC behaves differently on magnetic resonance imaging (MRI) than FA. It is speculated that their margins, T2-weighted imaging (T2WI) signal intensity, the presence or absence of peritumoral edema, dynamic enhancement features, and dispersion characteristics differ somewhat from those of FA. In this study, MRI images of 37 patients with TNBCs and 36 patients with FAs were retrospectively analyzed to investigate the value of MRI morphological manifestations, dynamic contrast-enhanced magnetic resonance imaging (DCE-MRI) parameters, and apparent diffusion coefficient (ADC) in the differential diagnosis of TNBC and FA, as well as the validation of the hypotheses in this paper. We present this article in accordance with the STARD reporting checklist (available at https://tcr.amegroups.com/article/view/10.21037/tcr-24-498/rc).

Highlight box

Key findings

- Morphological features, dynamic contrast-enhanced magnetic resonance imaging (MRI), and apparent diffusion coefficient (ADC) values were employed to distinguish between triple-negative breast cancer (TNBC) and fibroadenoma (FA) masses with a maximum diameter of less than 3 cm.

What is known and what is new?

- Imaging parameters derived from MRI play a crucial role in distinguishing between TNBC and FA.
- This study represents the first attempt to establish a multiparametric model based on MRI features for distinguishing between TNBC and FA masses with a maximum diameter of less than 3 cm.

What is the implication, and what should change now?

- Breast MRI, which has multi-parameters and functional imaging including MRI morphology, internal enhancement features, time-intensity curve, and ADC values, has great potential in preoperative differentiation of TNBC and FA.

Methods

Patients

The study was conducted in accordance with the Declaration of Helsinki (as revised in 2013). The study was approved by the Ethics Committee of the First Affiliated Hospital of Soochow University (No. [2024] 315) and informed consent was taken from all the patients. All patients were examined and treated at the First Affiliated Hospital of Soochow University. A total of 212 patients, aged from 20 to 68 years, with mass lesions were examined with breast-MRI before any intervention (biopsy, operation, or neoadjuvant chemotherapy) between January 2018 and December 2022. Inclusion criteria for the study were as follows: (I) breast MRI conducted within 1 week prior to surgery, with pathologically confirmed TNBC or FA diagnosis after surgery; (II) presence of a single TNBC lesion, with no previous history of puncture biopsy or surgery; (III) tumor diameter less than 3 cm. Exclusion criteria included (I) patients who had undergone biopsy, surgery, or neoadjuvant chemotherapy prior to scanning; (II) those with significant image artifacts, incomplete imaging sequences; (III) masses larger than 3 cm; (IV) or incomplete clinical data. The radiological results were blinded to the pathologists. The World Health Organization classification of breast cancer was used to classify the pathological diagnoses. Finally, 37 patients with TNBCs (histopathologically diagnosed as invasive breast cancers) and 36 patients with FAs (3 cases of multifocal FAs) were included, resulting in a total of 76 lesions (*Figure 1*).

MRI scanning

MRI was performed on Siemens MRI (MAGNETOM Skyra 3.0-T, Germany) with a unique 8-channel phased-array breast coil. Patients were placed in prone position. The MRI sequences included axial T1WI [repetition time (TR) =6 ms, echo time (TE) =2.5 ms, section thickness =1.2 mm, matrix size =320×320, field of view (FOV) =350×350 mm^2], axial fat-suppressed T2WI [TR =4,490 ms, TE =53 ms, inversion time (TI) =230 ms, section thickness =4 mm,

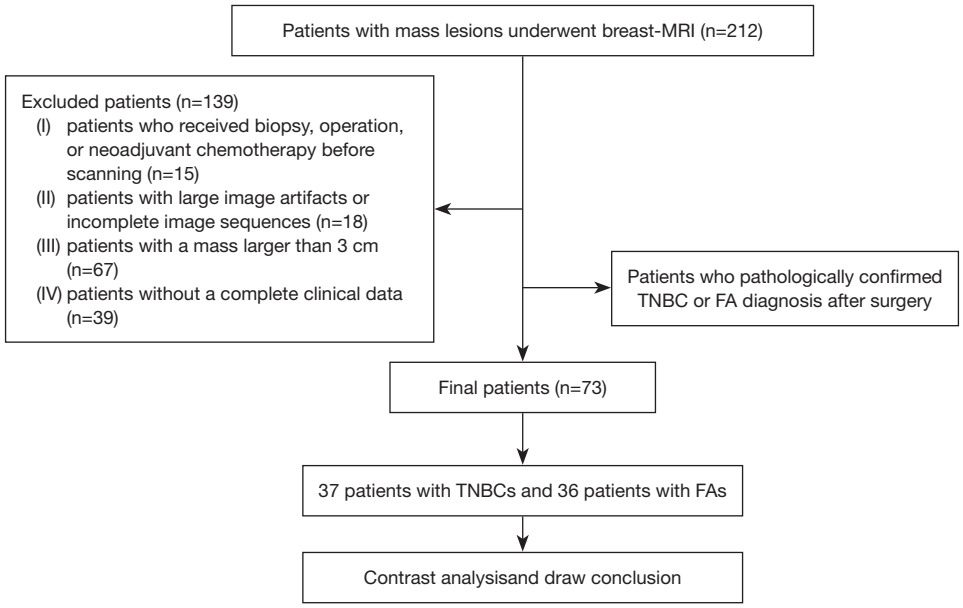

Figure 1 Flowchart of the patient selection and exclusion criteria. MRI, magnetic resonance imaging; TNBC, triple-negative breast cancer; FA, fibroadenoma.

matrix size =320×320, FOV =350×350 mm^2], diffusion-weighted imaging (DWI) (TR =10,400 ms, TE =53 ms, b=0.800 s/mm^2, section thickness =4 mm, matrix size =128×128, FOV =350×350 mm^2) and DCE-MRI. DCE-MRI using a three-dimensional volumetric interpolation breath-hold sequence (TR =4.5 ms, TE =1.7 ms, section thickness =1.2 mm, matrix size =320×320, FOV =350×350 mm^2). After an intravenous injection of a 0.1 mmol/kg dose of contrast agent (Gadolinium-DTPA) at a rate of 3 mL/s, five post-contrast DCE-MRI sequence scans were acquired starting 60 s after injection of the contrast agent at 60 s intervals. Gadolinium-DTPA (0.5 mmol/mL, Bayer) was power-injected at a dose of 0.1 mmol/kg body weight and a flow rate of 2.6 mL/s, followed by a 15 mL saline flush.

MRI analysis

DCE-MRI findings were retrospectively, individually reviewed, and evaluated by two radiologists with more than 10 years of experience with breast imaging, and the diagnosis was agreed upon through consultation. The data were processed using MeanCurve software on a Syngo MMWP post-processing workstation (version VE40B). The MRI morphological manifestations, DCE-MRI parameters, and ADC values were observed and measured with reference to the latest version of the 2013 Breast Imaging-Reporting and Data System (BI-RADS) MRI. These include the shape of the lesion (oval, round, irregular), margin (circumscribed, irregular, spiculated), predominant signal intensity on T2WI (based on the surrounding glandular tissue, classified as low signal, iso signal, and high signal), T2WI low-signal segregation (line-like T2WI low-signal shadows within the mass), peritumoral edema (the presence of signal intensities surrounding the tumor as high as that of water on the T2WI sequences) (8), initial phase enhancement rate (slow, medium, fast), internal enhancement characteristics (homogeneous, heterogeneous, rim enhancement, dark internal septations), types of time-signal intensity curve (TIC) (I = persistent, II = plateau, III = washout) and ADC value of the lesion. The region of interest (ROI) included the most enhanced lesion regions on the DCE images while avoiding cystic or necrotic lesions, with a ROI area of 4–25 mm^2.

ADC values were measured by referring to axial T1WI enhancement and T2WI sequence images. Vessels, catheters, necrotic areas, and cystic regions were avoided during the process. ROIs were plotted on ADC maps, and measured three times, the mean value of three ROI measurements was obtained as the final ADC value.

Statistical analysis

Statistical analysis was performed using SPSS (v24.0; IBM

Corp., Armonk, NY, USA). Comparisons of characteristics between TNBC and FA were performed using independent *t* test (age, ADC value), Chi-squared test (shape, margin, predominant signal intensity on T2WI, T2WI low-signal segregation, peritumoral edema, initial phase enhancement rate, internal enhancement characteristics, types of TIC). All P values were two-sided, and P values <0.05 were considered statistically significant. The study also plotted a non-parametric method of ADC values of receiver operating characteristic (ROC) curve and analyzed its diagnostic efficiency.

Results

Seventy-three patients were included in the study, involving 37 TNBC patients (mean age: 45.22±10.41 years; range, 28–65 years) with 37 lesions and 36 FA patients (mean age: 30.41±8.41 years; range, 20–49 years) with 39 lesions. There were two FA patients with bilateral single breast mass and one patient with two masses in a single breast, thus there were a total of 39 FA lesions. The mean age of patients in the TNBCs was significantly higher than that of the FAs (P<0.001) (*Table 1*). No significant adverse events during MRI scans.

Morphological manifestations of TNBC and FA

There was no statistically significant difference in T2WI signal intensity between the TNBC and FA (P>0.05) (*Table 1*). TNBC lesions were observed to have significantly more irregular shape, irregular margin, and peritumoral edema than FA (P<0.05). Conversely, FA masses were observed to have significantly more T2WI low-signal segregation than TNBCs (P<0.05) (*Table 1*).

DCE-MRI characteristics of TNBC and FA

A statistically significant difference was observed in the initial phase enhancement rate and internal enhancement characteristics between TNBC and FA lesions (P<0.05) (*Table 1*). A statistically significant difference was observed between TNBC and FA lesions in terms of TIC type. TNBC lesions predominantly exhibited type II or type III (97.29%), while FA lesions showed mostly type I or type II (97.43%) (*Table 1*, *Figures 2,3*).

ADC values of TNBC and FA and ROC curve analysis

The mean ADC value in the TNBCs was (1.104±0.13) $\times10^{-3}$ mm^2/s, which was significantly lower than the mean ADC value of (1.613±0.16)$\times10^{-3}$ mm^2/s in the FA lesions (P<0.05) (*Table 1*). *Table 2* shows lesion types in relation to mean ADC values.

A ROC curve was plotted based on the mean ADC values (*Figure 4*), and the diagnostic threshold of mean ADC values for diagnosing TNBC was set at 1.239×10^{-3} mm^2/s. The area under the curve (AUC) was 0.997, with a sensitivity of 94.6% and a specificity of 100% (*Table 3*).

Discussion

In the present study, we found that breast MRI is useful to differentiate TNBCs from FAs, and TNBC lesions were observed to have significantly more irregular shape, irregular margin and peritumoral edema than FA. TNBC lesions showed mostly type II or type III of TIC. The mean ADC value in the TNBC was significantly lower than in FA.

TNBC is a subtype of breast cancer with a poor prognosis (9,10). Due to the lack of effective therapeutic targets and high recurrence rate, the overall survival of patients is poor. In recent years, the TNBC population tends to be younger (11), and the demand for breast-conserving surgery is gradually increasing (12). Preoperative neoadjuvant chemotherapy has a high pathological remission rate, making it an effective therapeutic tool (13). Tumor diameter <3 cm is the key to breast-conserving surgery (14). Therefore, early detection and accurate assessment of the type of tumor is crucial to choosing the best treatment option. When TNBC appears as an oval hypoechoic solid mass with posterior acoustic enhancement at ultrasound (US), it can be diagnosed as FA. The majority of TNBCs have rim enhancement on DCE-MRI. However, approximately one-third of TNBCs with rim enhancement may contain enhancing internal septa, which may be misinterpreted as internal septa associated with benign FA (6). Studies have compared MRI features of TNBC with non-TNBC and benign tumors (15,16), as well as US comparative study (17). However, there are few MRI comparative studies of TNBC <3 cm with FA. Therefore, this study focuses on the differential diagnostic value of MRI in TNBC with FA, both of which <3 cm.

Table 1 Comparison of DCE-MRI features and DWI between the TNBCs and FAs

Characteristics	TNBC (n=37)	FA (n=39)	t/χ^2	P
Age, years	45.22±10.41	30.41±8.41	6.873	<0.001*
Shape			47.860	<0.001*
Oval	3 (8.1)	21 (53.8)		
Round	3 (8.1)	16 (41.1)		
Irregular	31 (83.8)	2 (5.1)		
Margin			57.047	<0.001*
Circumscribed	6 (16.2)	38 (97.4)		
Irregular	21 (56.8)	1 (2.6)		
Spiculated	10 (27.0)	0 (0.0)		
Predominant signal intensity on T2WI			0.168	>0.99
Low-signal	4 (10.8)	5 (12.8)		
Iso signal	12 (32.4)	13 (33.4)		
High signal	21 (56.8)	21 (53.8)		
T2WI low-signal segregation			5.769	0.03*
Positive	1 (2.7)	7 (17.9)		
Negative	36 (97.3)	32 (82.1)		
Peritumoral edema			39.269	<0.001*
Positive	25 (67.6)	0 (0.0)		
Negative	12 (32.4)	39 (100.0)		
Initial phase enhancement rate			5.361	0.045*
Fast	36 (97.3)	31 (79.5)		
Medium	1 (2.7)	6 (15.4)		
Slow	0 (0.0)	2 (5.1)		
Internal enhancement characteristics			28.324	<0.001*
Homogeneous	1 (2.7)	18 (46.3)		
Heterogeneous	9 (24.3)	7 (17.9)		
Rim enhancement	24 (64.9)	7 (17.9)		
Dark internal septations	3 (8.1)	7 (17.9)		
Types of TIC			44.286	<0.001*
I	1 (2.7)	26 (66.7)		
II	12 (32.4)	12 (30.7)		
III	24 (64.9)	1 (2.6)		
ADC value ($\times10^{-3}$ mm^2/s)	1.104±0.13	1.613±0.16	−15.202	<0.001*

Data are presented as mean ± standard deviation or number (percentage). *, P<0.05, results are statistically significant. DCE-MRI, dynamic contrast-enhanced magnetic resonance imaging; DWI, diffusion-weighted imaging; TNBC, triple-negative breast cancer; FA, fibroadenoma; T2WI, T2-weighted imaging; TIC, time-signal intensity curve; ADC, apparent diffusion coefficient.

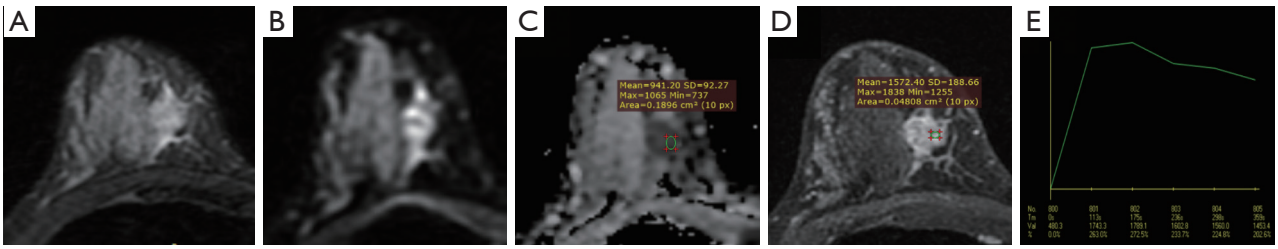

Figure 2 Breast MRI in TNBC female patient, aged 30 years old. (A) T2-dynamic sequence shows an irregular mass in the upper quadrant of the right breast, with an unsmooth edge and visible lobulation and spicules. (B) The DWI image shows a high signal intensity in the mass. (C) The ADC image using a 0.2 cm^2 circular ROI shows uneven low signal intensity of the tumor, with an average ADC value of approximately 0.941×10^{-3} mm^2/s. (D) Enhanced scan shows clustered circular enhancement. (E) TIC shows an outflow type (type III). MRI, magnetic resonance imaging; TNBC, triple-negative breast cancer; DWI, diffusion-weighted imaging; ADC, apparent diffusion coefficient; ROI, region of interest; TIC, time-signal intensity curve.

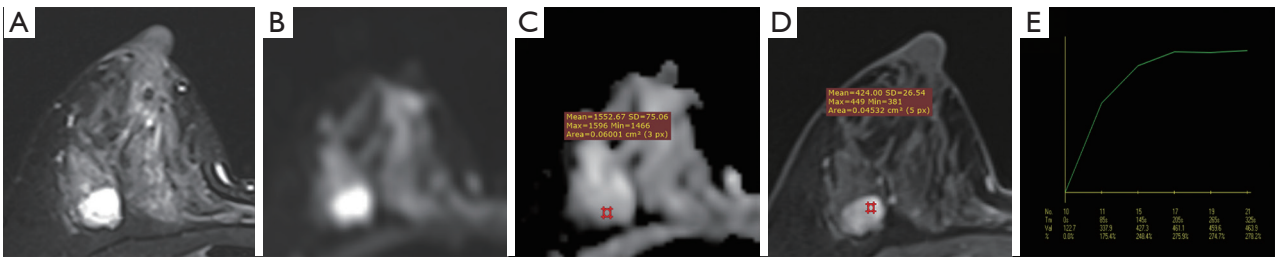

Figure 3 Breast MRI in FA female patient, aged 37 years old. (A) T2-dynamic sequence shows a circular mass in the upper outer quadrant of the right breast, with uniform high signal intensity and smooth edges. (B) The DWI image shows a high signal intensity in the mass. (C) The ADC image using a 0.06 cm^2 circular ROI shows high signal intensity of the tumor, with an average ADC value of approximately 1.552×10^{-3} mm^2/s. (D) Enhanced image display with uniform high signal. (E) TIC shows an inflow type (type I). MRI, magnetic resonance imaging; FA, fibroadenoma; DWI, diffusion-weighted imaging; ADC, apparent diffusion coefficient; ROI, region of interest; TIC, time-signal intensity curve.

Table 2 Lesion types in relation to mean ADC values

Disease	ADC ≤1.239×10^{-3} mm^2/s	ADC >1.239×10^{-3} mm^2/s	Total
TNBC	36	1	37
FA	1	38	39
Total	37	39	76

ADC, apparent diffusion coefficient; TNBC, triple-negative breast cancer; FA, fibroadenoma.

Lump-type TNBC often exhibits signs of benign breast tumors, such as small size, smooth margins (7,18), and regular morphology, which can make it difficult to distinguish them from FA in some cases. In this study, the TNBCs were mostly irregular (83.78%) and had irregular margins (83.78%), and some of them were round and

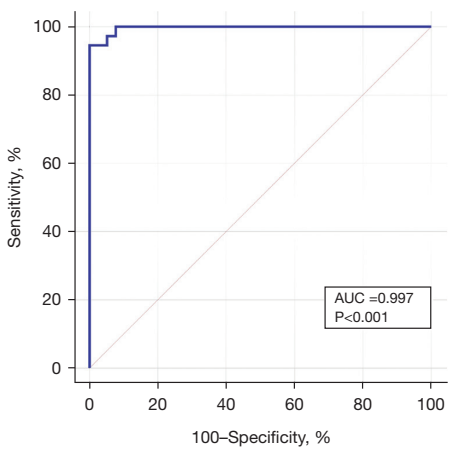

Figure 4 Receiver-operating characteristic curve of mean ADC values for TNBC and FA. AUC, area under the curve; ADC, apparent diffusion coefficient; TNBC, triple-negative breast cancer; FA, fibroadenoma.

Table 3 Diagnostic efficiency of TNBC and FA mean ADC values

	AUC (95% CI)	Diagnostic threshold value	Sensitivity	Specificity
ADC value ($\times 10^{-3}$ mm^2/s)	0.997 (0.946–1.000)	≤1.239	0.946	1.000

TNBC, triple-negative breast cancer; FA, fibroadenoma; ADC, apparent diffusion coefficient; AUC, area under the curve; CI, confidence interval.

oval (16.21%), whereas the FAs were mostly round and oval (94.87%), with clear margins. This may be related to the slow pushing growth of FA (19), so the lesions were relatively regular in shape and had clear borders with the surrounding tissues. In contrast, TNBC grew invasively and infiltrated the surrounding tissues to varying extents, resulting in irregularly shaped lesions with uneven edges.

High signal intensity on T2WI is an important feature of TNBC (7,16,20). TNBC grows rapidly and is prone to cystic degeneration, necrosis, and lymphocyte infiltration, resulting in increased T2WI signal. The high signal on T2WI of FA is due to the abundant cells in the tumor stroma and the occurrence of mucinous degeneration and edema (16,21,22). This study showed that T2WI in both TNBC and FAs was dominated by high signal intensity, as in previous studies (7,23,24).

T2WI low-signal segregation is a characteristic manifestation of FA (25), the underlying pathological basis for this phenomenon lies in the presence of collagen fiber bands. These collagen fibers exhibit low signal intensity due to their limited blood supply and the absence of hydrogen protons (26). Consistent with previous reports, 82.05% of the FAs in the present study showed T2WI low-signal segregation. Notably, we observed one case of TNBC that also exhibited T2WI low-signal segregation, which was histologically confirmed as fiber bands under hematoxylin and eosin (HE) staining.

Peritumoral edema is an important parameter for assessing the malignancy and predicting the prognosis of tumor (8,27,28). Park *et al.* (8) found that detailed histopathological characteristics of lymphovascular invasion, stromal fibrosis, and tumor necrosis as well as baseline clinicopathological characteristics of age and histologic grade were associated with peritumoral edema at breast MRI. TNBC is highly malignant and exhibits an invasive growth pattern, with peritumoral angiogenesis. The newborn naïve blood vessels have a greater permeability of the wall, resulting in edema of vascular origin. In this study, 67.56% of the TNBCs showed peritumoral edema, whereas no peritumoral edema was observed in the FAs. The above results suggest that peritumoral edema may be an indicative of a higher degree of tumor malignancy, which corresponds to the pathological basis of this sign (28).

The degree of tumor enhancement is mainly determined by the density of microvessels in the tumor tissue and the amount of contrast medium entering the tumor tissue. Previous studies have investigated that TNBC exhibits increased angiogenesis in the tumor periphery, central necrosis, and central desmoplasia (16,29). These features provide the basis for the internal enhancement features of TNBC, which are characterized by heterogeneous enhancement and rim enhancement (5). In this study, 24 cases (64.86%) showed early rim enhancement and 9 cases (24.32%) showed internal heterogeneous enhancement, followed by centripetal enhancement. The density distribution of microvessels in FA tumors was uniform and mainly showed gradual homogeneous enhancement. While 18 cases (50.00%) showed homogeneous enhancement, 7 cases (19.44%) showed internal dark segregation, which was considered to be caused by fibrous segregation inside the lesion (24,25). Therefore, the difference in internal enhancement characteristics between TNBC and FA is determined by their histopathological features.

TIC analysis can reflect the enhancement information within the tumor and analyze the neovascularization and perfusion characteristics of the tumor. A previous study has shown that the early enhancement rate of benign breast lesions is lower than that of malignant lesions (30), which may be related to the greater density of microvessels in malignant lesions, higher capillary permeability, and faster contrast inflow into the lesion. In this study, 97.30% and 79.49% of the lesions in the TNBCs and FAs, respectively, showed fast enhancement in initial phase. This difference was statistically significant between the two groups and consistent with the results of previous studies (31,32).

Kuhl *et al.* concluded that the TIC has important clinical value in identifying benign and malignant tumors (33). Breast cancer TIC curves mostly showed type II or type III, while benign tumors with less neovascularization mostly showed type I TIC curves. In this group of cases, the TNBC lesion was predominantly type II or III TIC (97.29%), whereas the FA lesion was predominantly type I

or type II (97.44%). The difference between the groups was statistically significant, consistent with previous literature report (34). Although both TNBC and FA are blood-rich lesions, TNBC is more invasive, with disorganized vascular structure and abundant neovasculature of varying degrees of malformation or immaturity. The contrast agent showed fast neovascularization, and the TIC mostly showed type III. On the other hand, FA lesions have well-developed blood-supplying vessels, minimal neovasculature, and slow signal change in the lesion area. The TIC curve is mostly type I.

DWI is a non-invasive imaging technique that is sensitive to the endogenous contrast of water molecule motion to tissue microstructural architecture and provides a quantitative parameter, the ADC value. Compared to benign tumors, malignant tumors have densely packed cells and small extracellular spaces, which limit the dispersion of water molecules and reduce the ADC value. Therefore, the ADC value can accurately identify benign and malignant breast lesions (35,36). A previous study has shown that the ADC value of breast cancer is lower than that of benign breast tumors (37). In this study, the mean ADC value of TNBCs was $(1.104\pm0.13)\times10^{-3}$ mm^2/s, which was significantly lower than that of the FAs, which was $(1.613\pm0.16)\times10^{-3}$ mm^2/s. When the diagnostic threshold was set at 1.239×10^{-3} mm^2/s, the AUC was 0.997, and the sensitivity and specificity of the diagnostic threshold were 94.6% and 100%, respectively. Therefore, the ADC value may be an effective value in differentiating TNBC from FA.

There are some limitations in this study. The small sample size of this study may have contributed to the 100% specificity of this diagnosis. The high degree of malignancy of TNBC, high cell densities, and low ADC values, while the T2WI mostly showed high signals, were not statistically different from those of the FAs. This may be related to the small sample size and subjective assessment bias. Therefore, it is necessary to quantitatively assess the T2WI signal intensity of TNBC and FA lesions in the future. In addition, the present study was a single-center study, and the study herein awaits clinical validation in a multicenter setting.

Conclusions

Breast MRI, which has multi-parameters and functional imaging including MRI morphology, internal enhancement features, TIC curves, and ADC values, has great potential in preoperative differentiation of TNBC and FA.

Acknowledgments

Funding: None.

Footnote

Reporting Checklist: The authors have completed the STARD reporting checklist. Available at https://tcr.amegroups.com/article/view/10.21037/tcr-24-498/rc

Data Sharing Statement: Available at https://tcr.amegroups.com/article/view/10.21037/tcr-24-498/dss

Peer Review File: Available at https://tcr.amegroups.com/article/view/10.21037/tcr-24-498/prf

Conflicts of Interest: All authors have completed the ICMJE uniform disclosure form (available at https://tcr.amegroups.com/article/view/10.21037/tcr-24-498/coif). The authors have no conflicts of interest to declare.

Ethical Statement: The authors are accountable for all aspects of the work in ensuring that questions related to the accuracy or integrity of any part of the work are appropriately investigated and resolved. The study was conducted in accordance with the Declaration of Helsinki (as revised in 2013). The study was approved by the Ethics Committee of the First Affiliated Hospital of Soochow University (No. [2024] 315) and informed consent was taken from all the patients.

References

1. Liedtke C, Mazouni C, Hess KR, et al. Response to Neoadjuvant Therapy and Long-Term Survival in Patients With Triple-Negative Breast Cancer. J Clin Oncol 2023;41:1809-15.

2. Yin L, Duan JJ, Bian XW, et al. Triple-negative breast cancer molecular subtyping and treatment progress. Breast Cancer Res 2020;22:61.
3. Cai L, Sidey-Gibbons C, Nees J, et al. Ultrasound Radiomics Features to Identify Patients With Triple-Negative Breast Cancer: A Retrospective, Single-Center Study. J Ultrasound Med 2024;43:467-78.
4. Liu Z, Yu B, Su M, et al. Construction of a risk stratification model integrating ctDNA to predict response and survival in neoadjuvant-treated breast cancer. BMC Med 2023;21:493.
5. Szep M, Pintican R, Boca B, et al. Multiparametric MRI Features of Breast Cancer Molecular Subtypes. Medicina (Kaunas) 2022;58:1716.
6. Schopp JG, Polat DS, Arjmandi F, et al. Imaging Challenges in Diagnosing Triple-Negative Breast Cancer. Radiographics 2023;43:e230027.
7. Uematsu T, Kasami M, Yuen S. Triple-negative breast cancer: correlation between MR imaging and pathologic findings. Radiology 2009;250:638-47.
8. Park NJ, Jeong JY, Park JY, et al. Peritumoral edema in breast cancer at preoperative MRI: an interpretative study with histopathological review toward understanding tumor microenvironment. Sci Rep 2021;11:12992.
9. Almansour NM. Triple-Negative Breast Cancer: A Brief Review About Epidemiology, Risk Factors, Signaling Pathways, Treatment and Role of Artificial Intelligence. Front Mol Biosci 2022;9:836417.
10. Bianchini G, De Angelis C, Licata L, et al. Treatment landscape of triple-negative breast cancer - expanded options, evolving needs. Nat Rev Clin Oncol 2022;19:91-113.
11. Zins K, Peka E, Miedl H, et al. Association of the Telomerase Reverse Transcriptase rs10069690 Polymorphism with the Risk, Age at Onset and Prognosis of Triple Negative Breast Cancer. Int J Mol Sci 2023;24:1825.
12. Li Y, Chen H, He J, et al. The outcome of neoadjuvant chemotherapy and the current trend of surgical treatment in young women with breast cancer: A multicenter real-world study (CSBrS-012). Front Public Health 2023;11:1100421.
13. Mittendorf EA, Zhang H, Barrios CH, et al. Neoadjuvant atezolizumab in combination with sequential nab-paclitaxel and anthracycline-based chemotherapy versus placebo and chemotherapy in patients with early-stage triple-negative breast cancer (IMpassion031): a randomised, double-blind, phase 3 trial. Lancet 2020;396:1090-100.
14. Jain U, Kothari A, Joshi S, et al. Breast conserving surgery revisited: a narrative review. Ann Breast Surg 2022;6:35.
15. Ohashi A, Kataoka M, Iima M, et al. A multiparametric approach to predict triple-negative breast cancer including parameters derived from ultrafast dynamic contrast-enhanced MRI. Eur Radiol 2023;33:8132-41.
16. Matsuda M, Tsuda T, Ebihara R, et al. Triple-negative breast cancer on contrast-enhanced MRI and synthetic MRI: A comparison with non-triple-negative breast carcinoma. Eur J Radiol 2021;142:109838.
17. Du Y, Zha HL, Wang H, et al. Ultrasound-based radiomics nomogram for differentiation of triple-negative breast cancer from fibroadenoma. Br J Radiol 2022;95:20210598.
18. Youk JH, Son EJ, Chung J, et al. Triple-negative invasive breast cancer on dynamic contrast-enhanced and diffusion-weighted MR imaging: comparison with other breast cancer subtypes. Eur Radiol 2012;22:1724-34.
19. Ajmal M, Khan M, Van Fossen K. Breast Fibroadenoma. 2024.
20. Yuen S, Monzawa S, Yanai S, et al. The association between MRI findings and breast cancer subtypes: focused on the combination patterns on diffusion-weighted and T2-weighted images. Breast Cancer 2020;27:1029-37.
21. Sharma S, Nwachukwu C, Wieseler C, et al. MRI Virtual Biopsy of T2 Hyperintense Breast Lesions. J Clin Imaging Sci 2021;11:18.
22. El-Sawy Deif Allah NS, Abdallah RH, Hassan MS, et al. Role of diffusion weighted imaging with background body signal suppression (DWIBS) in diagnosis of breast masses and correlation with histopathological findings. Egypt J Radiol Nucl Med 2024;55:95.
23. Westra C, Dialani V, Mehta TS, et al. Using T2-weighted sequences to more accurately characterize breast masses seen on MRI. AJR Am J Roentgenol 2014;202:W183-90.
24. Tsuchiya M, Masui T, Terauchi K, et al. MRI-based radiomics analysis for differentiating phyllodes tumors of the breast from fibroadenomas. Eur Radiol 2022;32:4090-100.
25. Igarashi T, Ashida H, Morikawa K, et al. Use of BI-RADS-MRI descriptors for differentiation between mucinous carcinoma and fibroadenoma. Eur J Radiol 2016;85:1092-8.
26. Nunes LW, Schnall MD, Orel SG, et al. Correlation of lesion appearance and histologic findings for the nodes of a breast MR imaging interpretation model. Radiographics 1999;19:79-92.
27. Harada TL, Uematsu T, Nakashima K, et al. Is the presence of edema and necrosis on T2WI pretreatment

breast MRI the key to predict pCR of triple negative breast cancer? Eur Radiol 2020;30:3363-70.
28. Cheon H, Kim HJ, Kim TH, et al. Invasive Breast Cancer: Prognostic Value of Peritumoral Edema Identified at Preoperative MR Imaging. Radiology 2018;287:68-75.
29. Xu R, Yu D, Luo P, et al. Do Habitat MRI and Fractal Analysis Help Distinguish Triple-Negative Breast Cancer From Non-Triple-Negative Breast Carcinoma. Can Assoc Radiol J 2024;75:584-92.
30. Qi X, Wang W, Pan S, et al. Predictive value of triple negative breast cancer based on DCE-MRI multi-phase full-volume ROI clinical radiomics model. Acta Radiol 2024;65:173-84.
31. Agrawal G, Su MY, Nalcioglu O, et al. Significance of breast lesion descriptors in the ACR BI-RADS MRI lexicon. Cancer 2009;115:1363-80.
32. Ferré R, Aldis A, AlSharif S, et al. Differentiation of Fibroadenomas and Pure Mucinous Carcinomas on Dynamic Contrast-Enhanced MRI of the Breast Using Volume Segmentation for Kinetic Analysis: A Feasibility Study. AJR Am J Roentgenol 2016;206:253-8.
33. Kuhl CK, Mielcareck P, Klaschik S, et al. Dynamic breast MR imaging: are signal intensity time course data useful for differential diagnosis of enhancing lesions? Radiology 1999;211:101-10.
34. Schnall MD, Blume J, Bluemke DA, et al. Diagnostic architectural and dynamic features at breast MR imaging: multicenter study. Radiology 2006;238:42-53.
35. Saccenti L, Mellon CM, Scholer M, et al. Combining b2500 diffusion-weighted imaging with BI-RADS improves the specificity of breast MRI. Diagn Interv Imaging 2023;104:410-8.
36. Tezcan S, Ozturk FU, Uslu N, et al. The Role of Combined Diffusion-Weighted Imaging and Dynamic Contrast-Enhanced MRI for Differentiating Malignant From Benign Breast Lesions Presenting Washout Curve. Can Assoc Radiol J 2021;72:460-9.
37. Fang J, Zhang Y, Li R, et al. The utility of diffusion-weighted imaging for differentiation of phyllodes tumor from fibroadenoma and breast cancer. Front Oncol 2023;13:938189.

Cite this article as: Wei Z, Chen X, Yang Y, Yang L, Ma X. The potential role of breast MRI in evaluation of triple-negative breast cancer and fibroadenoma of less than 3 cm. Transl Cancer Res 2024;13(8):4042-4051. doi: 10.21037/tcr-24-498

